Current Indian Science

Content list available at: https://currentindianscience.com

RESEARCH ARTICLE

Assembling, Computational and Experimental Insight of Self-assembled Carbo Benzyl oxy-L-Alanyl-L-Valine Benzyl Ester: A Novel Free Radical Scavenger and Photo Therapeutic Nano Molecular System

M. Sivanathan[1], R. Naveenkumar[1] and B. Karthikeyan[1,*]

[1]*Department of Chemistry, Annamalai University, Annamalai Nagar, 608002, India*

Abstract:

Introduction:

This work investigates the synthesis of self-assembled novel carbo benzyl oxy - L - alanyl - L - valine benzyl ester (CBAVBE).

Methods:

Thorough studies of the morphology, optical, and structural investigations by UV-Visible, UV-DRS, FT-IR, FT-Raman, HR-TEM, and FE-SEM are used to characterize the self-assembled CBAVBE and computational studies also investigated. The anti-oxidant capability of carbo benzyl oxy - L - alanyl - L - valine benzyl ester is evaluated after self-assembly.

Results:

FT-IR and Raman analysis have proven that specific chemical bonds exist in the self-assembled CBAVBE. FE-SEM analysis clearly confirms that the CBAVBE is fibrous in nature, and the collected images clearly show the CBA assembly VBE to be well aggregated. The docking analysis suggests that the CBAVBE molecule has inhibitory action against brain and lung cancer protein but biological study is needed to validate the results. An antioxidant study reveals the potential of the selected CBAVE as a notable biomarker.

Conclusion:

A new class of self-assembled peptide nano self-assemblies have been marked as a discovery that could be used to treat a variety of diseases.

Keywords: Self - Assembled Benzyl ester, DPPH, Free radical scavenging, Docking studies, CBAVE, DNA damage.

Article History	Received: March 01, 2024	Revised: June 29, 2024	Accepted: July 09, 2024

1. INTRODUCTION

Unstable radicals have a tendency to form stable interactions with biological macromolecules, causing protein and DNA damage. The discovered antioxidant potential motivates research into cancer protein docking, particularly those found in lung cancer. Oxidant stress, characterized by high levels of oxygen radicals, is a major contributor to vascular endothelial dysfunction and has been linked also development to a number of vascular illnesses, along with diabetes and atherosclerosis. Nutritional variables may be essential in the regulation of endothelial function as well as lowering oxidative stress-related illness, according to recent studies. L-alanine, L-glycine, and L-serine are three amino acids that have been demonstrated to protect kidney tubular cells and hepatocytes from oxidative, metabolic, and chemical stress. Furthermore, it has been revealed that endothelial cell death induced by reactive oxygen species or elevated calcium levels can be reduced significantly by L-alanine and structurally similar amino acids [1].

The impact of type and six independent antioxidant activity tests were used to explore the effects of amino acid side chains on the antioxidant activities of tri peptides having two tyrosine's and tri peptides containing two histidine's. Peptides' antioxidant properties are determined by characteristics, chemical and physical sequencing, and structure of amino acids [2, 3]. Peptide chains with bioactivity usually contain two to twenty amino acid residues, containing a high proportion of hydrophobic amino acids. Antioxidant activity is found in almost every bioactive peptide present in Tyr, Phe, Leu, Ala,

* Address correspondence to this author at the Department of Chemistry, Annamalai University, Annamalainagar 608002, India; Tel: +919842491114; E-mail: bkarthi_au@yahoo.com

Ile, Val, Lys, Cys, Met, and His. Many bioactive peptides possess antioxidant properties. They can scavenge and neutralize ROS directly, reducing oxidative stress in cells and tissues. This helps prevent oxidative damage to biomolecules such as proteins, lipids, and DNA, which can lead to various chronic diseases, including cardiovascular diseases, cancer, and neurodegenerative disorders. Purification and isolation processes can enhance the bioavailability and stability of bioactive peptides, ensuring that they reach their target sites in the body in active form. This improves their effectiveness in combating oxidative stress and related health risks. The isolation and purification of bioactive peptides from natural sources offer promising strategies to mitigate health risks associated with ROS by directly scavenging free radicals, modulating oxidative stress pathways, and enhancing cellular antioxidant defences. These properties make bioactive peptides potential candidates for therapeutic interventions targeting oxidative stress-related diseases [4].

The sequence of signals is required by mitochondria for a effective transport and processing of proteins. MnSOD's signal sequence has an alanine-to-valine polymorphism (Ala16Val), often known as the –9 position, causes the protein's helical shape to change conformation, according to indirect evidence. Although other investigations have found that this polymorphism has different and opposing functional effects, this change may affect the effectiveness of the Valine isoform of the protein's trafficking into mitochondria [5]. Recent advancements in the production of fibrillizing peptide gels as well as their *in vitro* and physiological settings, are discussed in this research article. We will then go through some of the promising recent *in vivo* results for this class of materials, as well as some of the hurdles that remain for using them in biomedical applications [6]. Atherosclerotic, arthritic, diabetic, cataract genesis, muscular dystrophy, respiratory dysfunction, inflammatory disorders, ischemia-reperfusion tissue injury, and neurological illnesses such as Alzheimer's disease are all connected to lipid and cellular macromolecule changes caused by free radicals. Lipid peroxidation in foods is a key cause of food quality things that impacts flavor, texture, and appearance, as well as nutritional content, and may cause disease after consumption [7].

Antioxidants are chemicals that prevent or reduce cellular damage by blocking or quenching free radical activity. Though antioxidant activity differs by species, antioxidant defenses are present in all of them. Antioxidants can be present in both intracellular and extracellular contexts, they can be found in both enzymatic and non-enzymatic forms. Normal metabolic responses, increased exposure to the environment, and increasing amounts of food ROS (reactive oxygen and nitrogen species) are produced by all xenobiotics (RNS). Antioxidants can be categorized in a number of ways. Based on how they work, they are classified as enzymatic or nonenzymatic antioxidants. Antioxidant enzymes break down and eliminate free radicals. Antioxidants come in two forms: water-soluble and lipid-soluble. Water-soluble antioxidants can be found in cellular fluids like cytosol and cytoplasmic matrix. Antioxidants that are soluble with lipids are usually found in cell membranes [8]. Furthermore, to achieve a high-quality final product, dry-cured ham in Spain is made with ripening, salting, and post-salting. During the ripening process, the proteolytic action of muscle endogenous end peptidases, peptide peptidases, and amino peptidases, which are important in favoring the sensory qualities and nutritional value of ham, generates a huge amount of free amino acids and peptides. It has been shown that dry-cured ham is a natural source of bioactive peptides with antioxidant properties by using improved mass spectrometry methods and peptidomic approaches. Moreover, due to their vast spectrum of biological activity, peptides from enzymatic hydrolysates of dietary proteins have recently caught the attention of food scientists. These hydrolysates are known as food-borne bioactive peptides, and the protein content and Peptide sequencing fragments are produced frequently but are not the same as bigger dietary proteins. Antioxidants, hypertensive, immune-modulatory, and cholesterol-lowering peptide fragments from the same dietary protein may have diverse physiological effects. Despite this and their structures, many active peptides in oligo peptides are currently unknown, and there is no public database describing peptide structure–function connections.

As a result, bioactive peptides with specific activities isolated and purified, and their structures must be determined. Additionally, because of their unpaired electrons, reactive oxygen species (ROS) are formed by many physiological processes. ROS may cause a wide range of health issues in the body, including cardiovascular and cerebrovascular illness, arthritis, diabetes, skin disorders, ageing, and even cancer [9, 10]. As a result, knowing the antioxidant content and efficacy in foods is crucial for food preservation and oxidative damage protection, as well as avoiding unwanted changes and loss of economic and nutritional value. This entails developing a rapid method for determining the antioxidant potential of various foods [11 - 16]. The goal of this study is to investigate the self-assembly of an ester as peptides in a liquid medium and its anti-cancer activity using various techniques.

2. MATERIALS AND METHODS

2.1. Materials

Carbo Benzyl oxy-L-Alanyl-L-Valine benzyl ester. Ethanol, DPPH, Disodium hydrogen phosphate, monosodium hydrogen phosphate, and Ascorbic acid were procured from Sigma Aldrich. All of the compounds were used in the same manner.

2.2. Methods

2.2.1. Preparation of Self-assembled CBAV Benzyl Ester

In a 100 mL reaction vessel, the following ingredients are combined. Ten ml of Carbo Benzyl oxy -L-Alanyl-L-Valine benzyl ester aqueous solution is added. The solution-containing reaction vessel was placed in a pre-warmed silicon oil bath (65^{o}C) and gently stirred for 30 minutes before being removed from the heat. The solution was then allowed to cool at room temperature for 3 hours with moderate stirring [17]. Furthermore, using a silicon oil bath provides stable and uniform heating, ensuring that all parts of the reaction mixture are exposed to the same temperature, which contributes to consistent yields across experiments. The temperature of 65°C

is often chosen based on the reaction kinetics and the stability of the reagents and intermediates involved. At this temperature, the reaction typically proceeds at a rate that balances both the speed of the reaction and the selectivity toward the desired product formation. Moreover, by maintaining a specific temperature (in this case, 65°C), the reaction conditions are set to minimize side reactions that could lead to undesired by-products or the decomposition of sensitive intermediates.

2.2.2. Preparation of DPPH Assay

A solution of 0.1mM DPPH (4 mg in 100 ml ethanol) was prepared for the assay.

2.2.3. Theoretical Calculations

Simulation and optimization of the ground state geometry CBAV benzyl ester was performed using the Gaussian 03W software, DFT technique at the Beck, three-parameter, Lee-Yang-Parr(B3LYP)/LanL2DZ level of theory [18]. The B3LYP functional fields have proven consistent in forecasting energy gap values for tiny clusters in previous studies of self-assembled CBAVBE. DOS plots were plotted with the Gaussum package [19 - 27].

2.2.4. Docking Studies

Ground state geometry optimization and simulation CBAV benzyl ester were auto-docked by the MGL Tools 1.5.6 program's graphical user interface [20, 21]. It is already known that Auto Dock software is a simulation software used to predict the interaction of ligands with molecules, or it is an ideal procedure to find the global minimum energy of interaction during protein-ligand docking. The Multiwfn [22] and Program VMD 9.1 [21, 23, 25] Reduced Density Gradient was created using the software (RDG).

3. RESULT AND DISCUSSION

3.1. Visible Spectroscopy (UV)

Spectra of UV-vis absorbency of CBAVBE is shown in Fig. (**1a**). The wide optical absorption peak at 260 nm is noted for the possible electronic transition.to n-π* transition.

3.2. UV- DRS

Fig. (**1b**). shows the UV – DRS of the self-assembled CBAVBE. In the UV-vis range, CBAVBE has a much higher reflectivity. This is due to the fact that the CBAVBE has a high absorbance in the selected region. CBAVBE's UV-DRS is expressed in F (R). The kubelka-munk algorithm F(R) = (1-R)2/2R was used to determine the F(R) values from the recorded reflectance (R), where F(R) is the kubelka-munk value and R is the diffuse powder reflection. The calculated band gap denotes the energy differences between the top of the valence band, which is full of electrons, and the bottom of the conduction band, which is empty. The plot represents $[F(R)hv]^2$ *versus* photon energy (hv) provides the direct band gap of the self-assembled CBAVBE as 2.506 eV. High absorbance ensures that CBAVBE can detect low levels of incident light, enhancing the sensitivity and reliability of photodetectors in various applications, including environmental monitoring and optical communications. The ease of integration into device architectures and compatibility with existing manufacturing processes will also influence its real-world applicability.

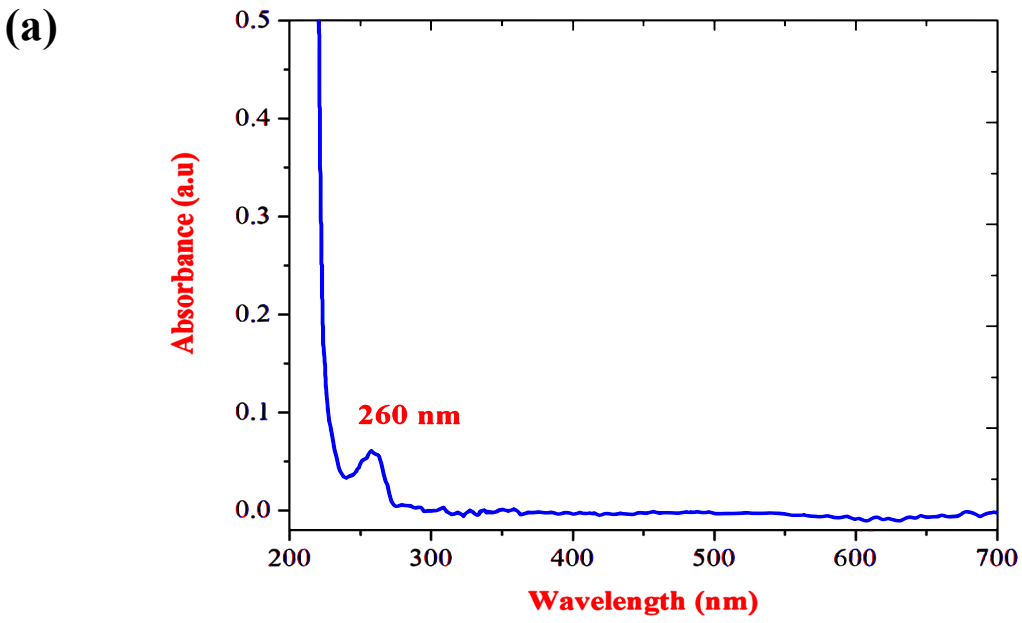

Fig. (1a). UV – Visible spectroscopy of CBAVBE.

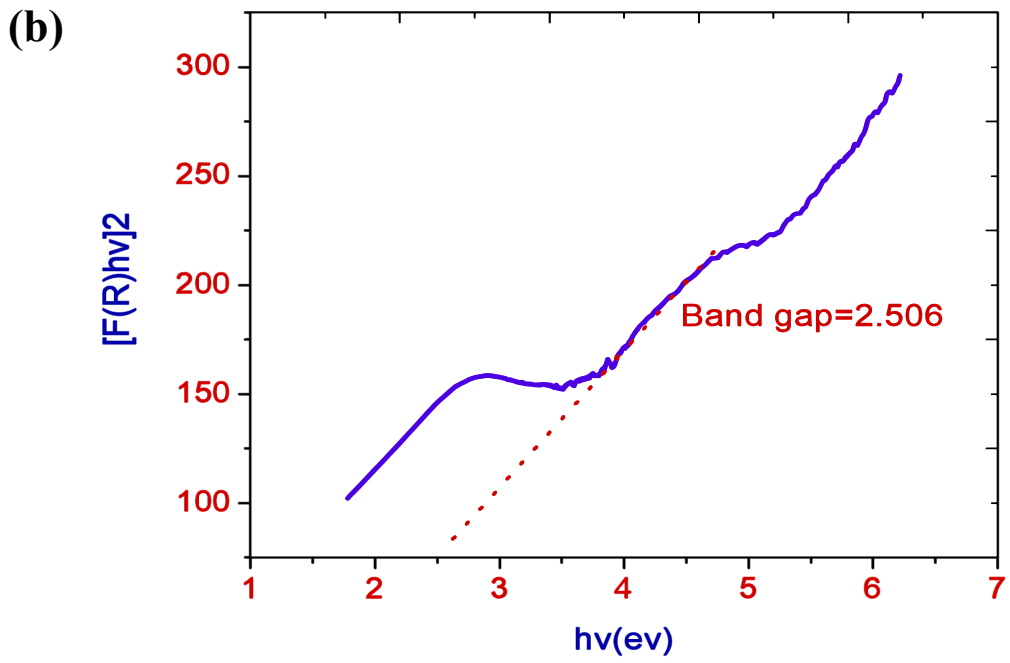

Fig. (1b). UV- DRS spectroscopy of CBABVE.

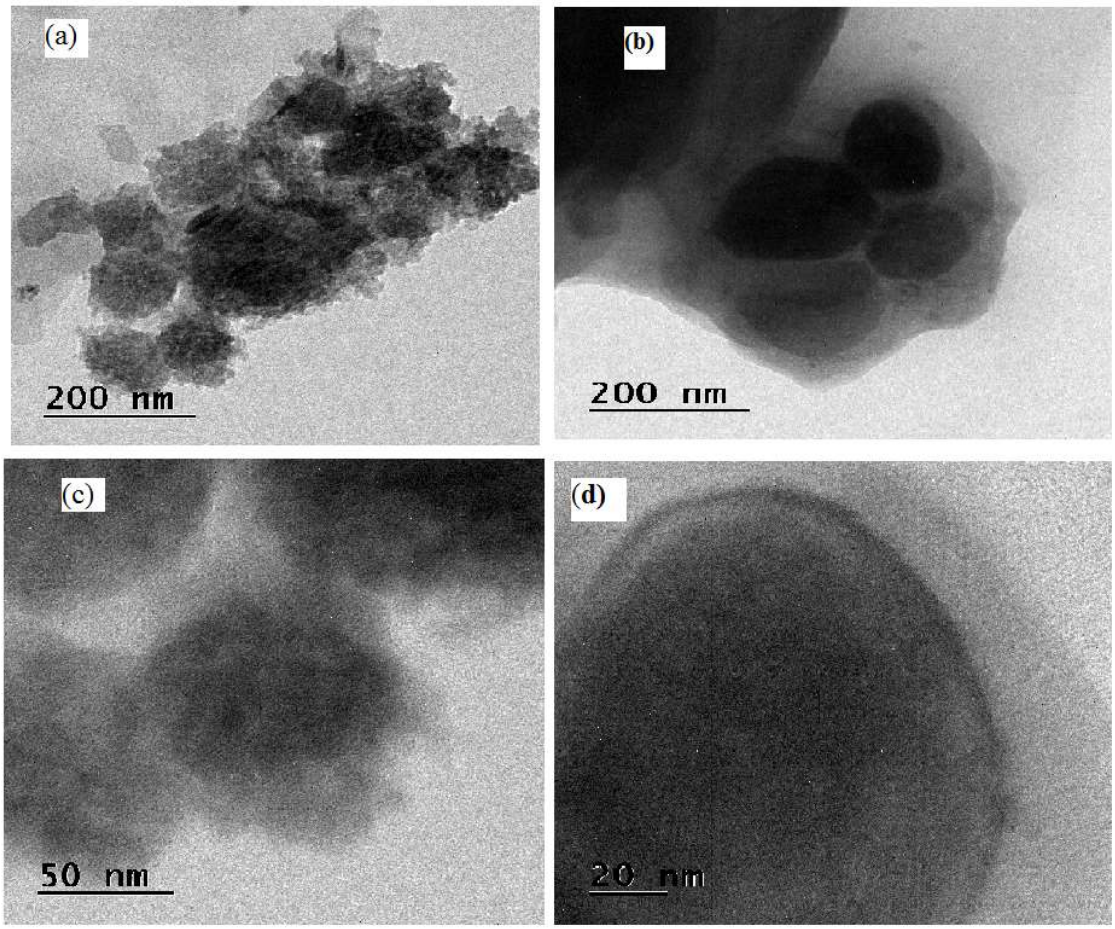

Fig. (2a-d). HR - TEM Analysis of self-assembled CBAVBE.

3.3. HR - TEM Analysis

The tube-like structure of the self-assembly is examined using HR-TEM analysis and was assembled by CBAVBE. HR-TEM images of CBAVBE at various magnifications are shown in (Fig. **2a-d**). This analysis clearly demonstrates that the self-assembly shows a tubular shape, and the collected images clearly illustrate the CBAVBE, which is highly aggregated with time.

3.4. FE - SEM Analysis

FE-SEM investigation of the tubular structure self-assembled CBAVBE displays SEM images of CBAVBE at various magnifications. This analysis clearly confirms that the CBAVBE is fibrous in nature, and the collected images clearly show that the CBA assembly VBE is well aggregated.

3.5. FT-IR Spectrum Analysis (Fourier Transform Infrared)

A frequency observed at 3440 cm^{-1} for NH stretching vibration, 1884 cm^{-1} for vibrations of C=O stretching (amide linkage), 1636 cm^{-1} for NH bending vibration, 1131 cm^{-1} for C-O stretching vibration (C-O-C), and 1096 cm^{-1} for C-N stretching vibration is assigned to CBAVBE in the FT-IR spectra shown in Fig. (**3**) The presence of several functional groups such as carbonyl, amino, amide, and ester groups is also shown by the FT-IR spectra of CBAVBE and the values are shown in Table **1a**.

3.6. Fourier Transform (FT- Raman) Spectral Analysis

The frequency of stretching observed at 3218 cm^{-1} for NH stretching vibration of CBAVBE is shown, while 2933 cm-1 is assigned to CH sym stretching vibration, 1590 cm^{-1} is attributed to CH asymmetric stretching vibration, 1455 cm^{-1} C=O stretching vibration is significant for cm-1, 1282 cm-1 is attributed to CH stretching vibration, and 1090 cm-1 is attributed to NH out of plane bending vibration. The presence of several functional groups, such as carbonyl, amino, amide, and ester groups, is also shown by the FT- Raman spectra of CBAVBE. The functional groups are provided in Table **1b**.

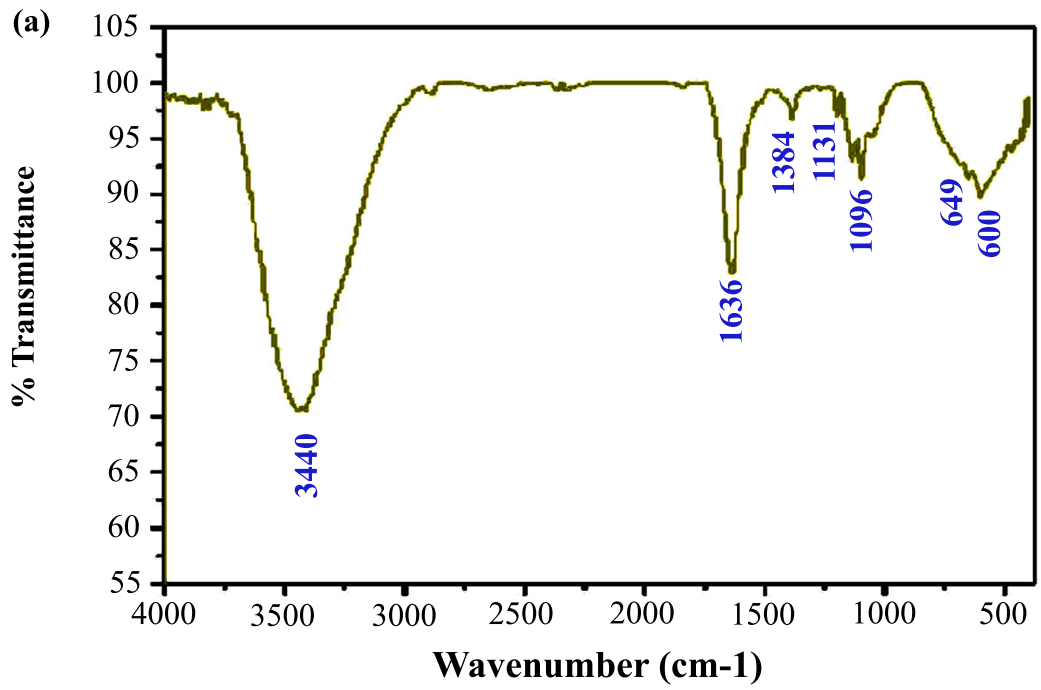

Fig. (3a). Experimental FT-IR spectral analysis of self-assembled CBAVBE.

Table 1a. Experimental FT – IR and selective computed Infrared vibrational frequencies of CBAVBE with their assignments.

S.No.	FT – IR (cm^{-1})	Computed IR (cm^{-1})	Assignments
1	1096	1051	C-N Stretching
2	1131	1116	C-O Stretching (C-O-C)
3	1636	1628	N-H bending
4	1884	1807	C=O Stretching (amide)
5	3340	3556	N-H Stretching

Table 1b. Experimental FT – Raman and selective computed Raman vibrational frequencies of CBAVBE with their assignments.

S. No.	FT – Raman(cm^{-1})	Computed Raman(cm^{-1})	Assignments
1	3218	3194	N- H Stretching
2	2933	3045	C- H Sym Stretching
3	1590	1648	C- H Asym Stretching
4	1455	1486	C=O Stretching
5	1282	1280	CH Stretching
6	1090	1090	CH bending

4. THEORETICAL STUDIES

4.1. Frontier Molecular Orbital's (FMO) Analysis

The CBAVBE's B3LYP/6-311G optimized structure and frontier molecular orbitals are shown in Fig. (**4a**, **b**). The molecular orbitals are made up of 200 valance electrons, with the highest occupied molecular orbital (HOMO) possessing anti-symmetric characteristics (A) and the lowest unoccupied molecular orbital (LUMO) possessing an energy of around -0.0294 amu. The atomic orbitals that are primarily contributing to the HOMO-LUMO can be plainly observed among the 100 molecular orbitals in Fig. (**4c**). ELUMO - HOMO = 2.0016 eV is determined to indicate the excitation energy gap between those two molecular orbitals.

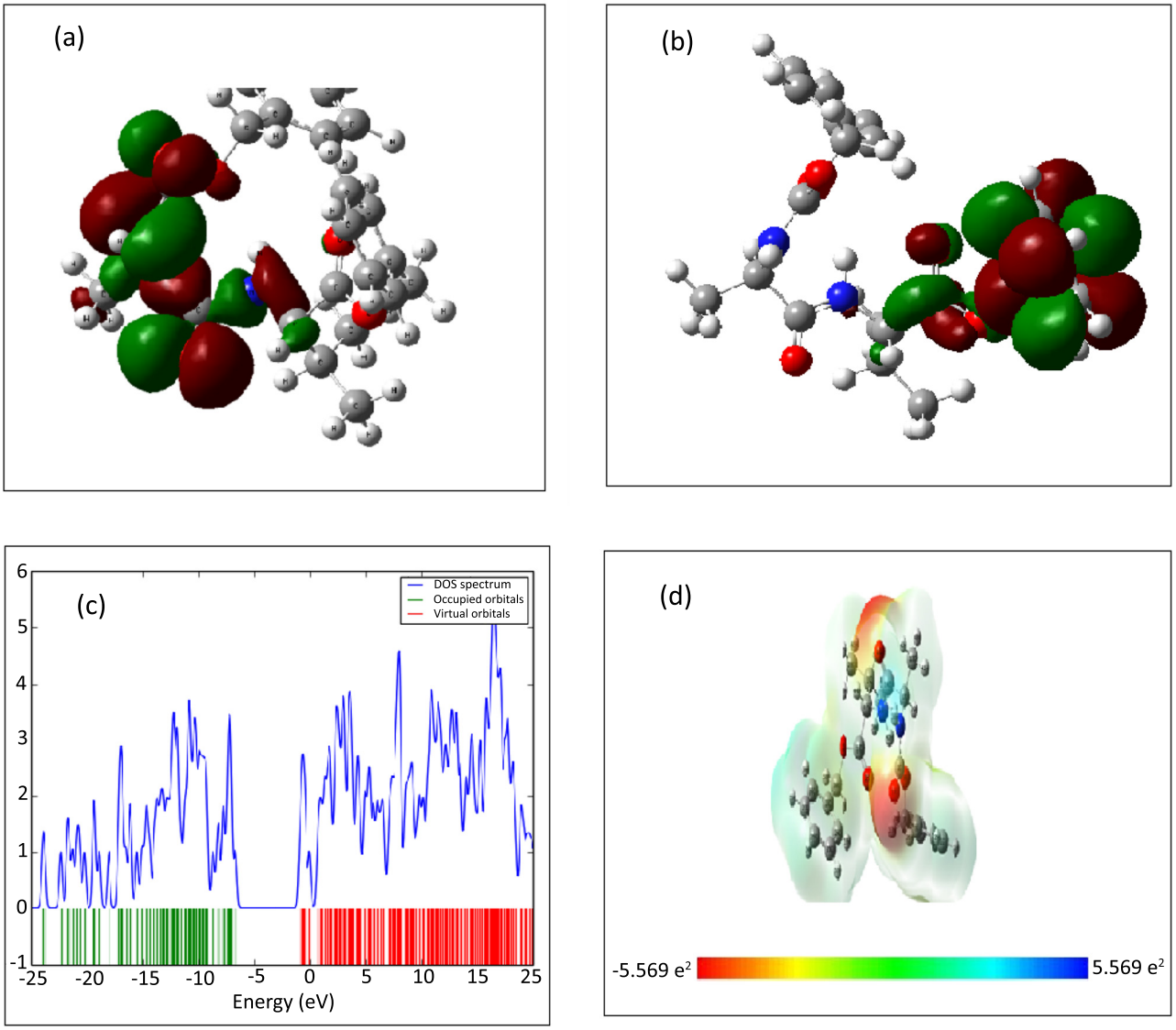

Fig. (4). (**a**) HOMO (**b**) LUMO (**c**) Density of state (**d**) molecular electrostatic potential of CBAVBE.

4.2. Density of State (DOS) Spectral Analysis

Fig. (**4d**). represents the electron density of states (DOS) of CBAVBE, which shows two characteristic peaks, both extending from 5.780 eV below and above the energy gap, respectively.

4.3. Analysis of Electrostatic Surface Potential (ESP) and Molecular Electrostatic Potential (MEP)

MEP analysis shows the time-invariant electric field charges on Carbo Benzyl oxy -L- Alanyl -L- Valine benzyl ester nanofibrous, and it indicates the most active positions (with higher electron-rich densities) in CBAVE nanofibrous. The oxygen atoms (O100 O150) of CBAVBE's carbonyl group are represented by orange areas (-5.569e-2). It demonstrates that electrophilic sites, such as oxygen atoms, are the most attacked sites. The MEP also depicts the reactivity of hydrogen bonding interactions, as well as electrophilic and nucleophilic attacks [21].

5. ANTI-OXIDANT STUDIES

The effects of the kind and quantity of amino acid side chains on the antioxidant activities of peptides containing two amino acids, such as alanine and valine, were studied. The assay is focused on determining how effective antioxidants are at scavenging free radicals. Furthermore, by obtaining a hydrogen atom from antioxidants, the odd electron of the nitrogen atom in DPPH is decreased [11]. The details are explained in the following sections.

5.1. Free Radical Scavenging Activity of DPPH

The DPPH free radical scavenging ability of the samples was measured using the method of Kedare *et al*. [11]. Furthermore, to summarize, 100 ml of 0.1 mmol/L DPPH in 95 percent ethanol was added to 100 ml of each sample at various concentrations (0.2, 0.4, 0.6, 0.8, and 1.0) mg/ml to maintain (PH 7.4 -9.0) while adding phosphate buffer, then the mixture was kept for 30 minutes in the dark at room temperature after shaking, and then the absorbance at 517 nm was measured. The calculation of scavenging activity was influenced by a number of factors.

$$\text{DPPH Scavenging \%} = [(Ao - A_1)/Ao] \times 100$$

Where A_1 is the absorbance of the mixtures and standard, and Ao is the absorbance of the control [11].

5.2. Comparison Free Radical Scavenging of DPPH with CBAVBE and Standard Ascorbic Acid

The anti-oxidant potential of CBAVBE compared with ascorbic acid. Even at low concentrations (0.2 ml), it shows effectiveness as an anti-oxidant.

5.3. Mechanism of Free Radical Scavenging

Furthermore, because the free electron is dispersed throughout the molecule, DPPH is a stable free radical that does not dimerize as the majority of other radicals do. The deep violet color is caused by delocalization; in an ethanol solution, it absorbs at 520 nm. The reduced form of DPPH is created when it is coupled with a molecule that can donate a hydrogen atom, and the violet color is gone [11]. Alanine has a non-polar side chain that consists of a methyl group ($-CH_3$). This methyl group can donate a hydrogen atom to free radicals, particularly those involved in lipid peroxidation reactions. Furthermore, by donating a hydrogen atom, alanine stabilizes and neutralizes the free radical, thereby preventing further oxidative damage to lipids. Valine also has a non-polar side chain with a longer hydrocarbon chain compared to alanine. This side chain can similarly donate hydrogen atoms to free radicals, albeit with potentially different efficiency due to its larger size and structural properties. The combined contribution of Alanine and Valine residues in a peptide determines its overall antioxidant capacity. Peptides with optimized sequences that maximize hydrogen atom donation and resonance stabilization properties of Alanine and Valine are likely to exhibit enhanced antioxidant activities against various types of free radicals. The antioxidant activities observed in peptides containing alanine and valine stem from their ability to donate hydrogen atoms to free radicals, thereby neutralizing their reactivity and preventing oxidative damage. The specific mechanisms include hydrogen atom donation, steric effects, resonance stabilization, and peptide sequence context, all of which contribute to variations in antioxidant activities observed in peptides containing these amino acids.

6. MOLECULAR DOCKING STUDIES

6.1. Docking and Hydrogen Bond Interaction

The PASS (Prediction of Activity Spectra) is an online tool that predicts molecular structure-activity and also reveals that the substance we have chosen is more effective against cancer disease, as shown in Table **2**. It is already known that Auto Dock software is simulation software used to predict the interaction of ligands with molecules, or it is an ideal procedure to find the global minimum energy of interaction during protein-ligand docking. The 3D crystal structure of brain and lung cancer protein was obtained from Protein Data Bank (PDB ID: 1QH4) and (PDB ID: 2ITO) with a resolution of 1.41 Å and 3.25 Å [12, 13]. The co-crystallized ligand and water molecules were removed to make the protein. Furthermore, Auto Dock Tools, a graphical user interface produced by MGL Tools 1.5.6, added all hydrogens, and Kollman charges were assigned to all atoms of the protein [14, 15]. All of the target protein's residues were mapped within the grid size of 120 Å x 120 Å x 120 Å points using Auto Grid 4 [16, 17]. The ligand structure was energy minimized using the Gaussian 09W program [18]. The hydrogen bonding pose diagram of protein-ligand of brain cancer and lung cancer is shown in Fig. (**5**). From that analysis, it shows that there is an interaction with the amino acid residue of ALA379 for brain cancer protein with a bond distance of 1.9 Å with a binding energy value of -2.86 Kcal/mol and GLN935, ARG932 for lung cancer protein with a bond length of 2.1 and 2.2 Å with a binding energy value of -2.80 Kcal/mol are shown in Table **3a** & **3b** and it was visualized using Pymol software [19]. The results show that it is a pure, strong hydrogen bond formation with the hydrogen bond distance of <3 Å. The protein-ligand interaction was visualized using the Discovery Studio Visualizer [19]. The results were used to examine the

energetically permissible zone in terms of amino acid residue. The blue region denotes the allowed region to the docking, indicating the binding energy strength, which is high during docking. The docking analysis suggests that the CBAVBE molecule has inhibitory action against brain and lung cancer protein, but a biological study is needed to validate the results.

Table 2. PASS Online prediction of CBAVBE compound.

[a]Pa	[b]Pi	Predicted Activity
0.936	0.003	Chymosin inhibitor
0.936	0.003	Saccharopepsin inhibitor
0.936	0.003	Acrocylindropepsin inhibitor
0.913	0.005	Polyporopepsin inhibitor
0.447	0.004	Cancer procoagulant inhibitor
0.211	0.040	Antineoplastic (endocrine cancer)
0.232	0.063	Antineoplastic (bone cancer)
0.275	0.135	Cancer associated disorders treatment
0.171	0.052	Antineoplastic (cervical cancer)
0.189	0.099	Antineoplastic (liver cancer)
0.191	0.147	Antineoplastic (brain cancer)

Note: [a]Pa represent probability to be active.
[b]Pi represents probability to be inactive.

Table 3a. Molecular docking results of CBAVBE molecule with different types of cancer protein targets.

Drug	Type of Cancer	Protein ID	Binding Energy (Kcal/mol)	Estimated Inhibition Constant Ki (μM)	RMSD
CBAVBE	Brain	1QH4	-2.86	8.04	78.46
	Lung	2ITO	-2.80	8.80	66.47

Table 3b. Summary of hydrogen bonding of CBAVBE molecule with different types of cancer protein targets.

Protein (PDB ID)	No. of Hydrogen Bond	Bonded Residues	Bond Distance (Å)
1QH4	1	Protein: A: ALA 379	1.9
2ITO	2	Protein: A: GLN 935 Protein: A: ARG 932	2.1 2.2

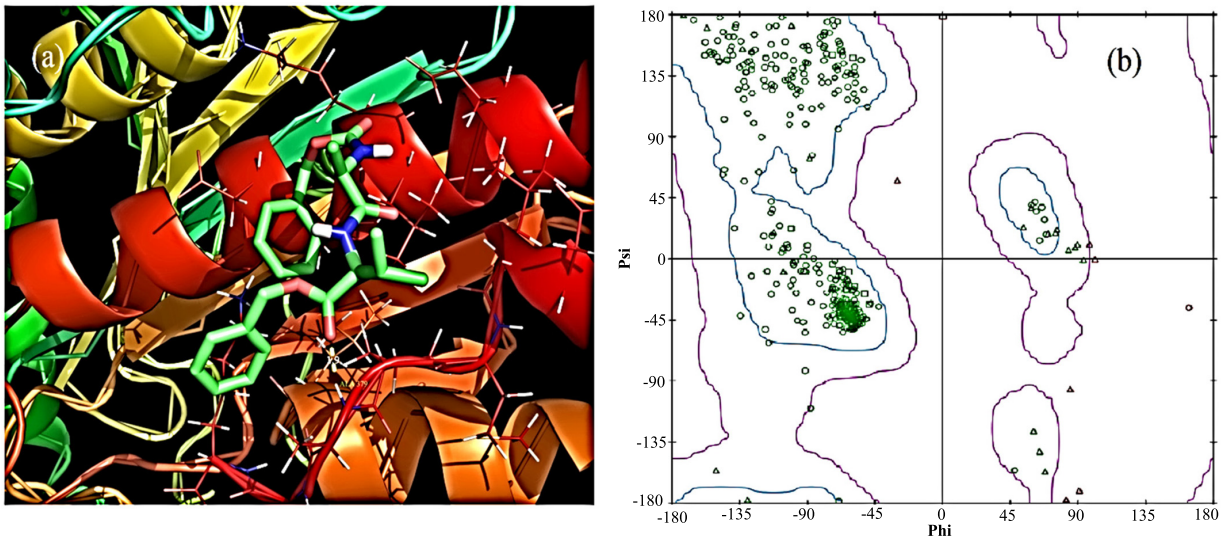

Fig. (5). (**a**) Docking and hydrogen bond interaction of Brain cancer (1QH4) protein with CBAVBE molecule.
(**b**) Graphical representation of Docking and hydrogen bond interaction.

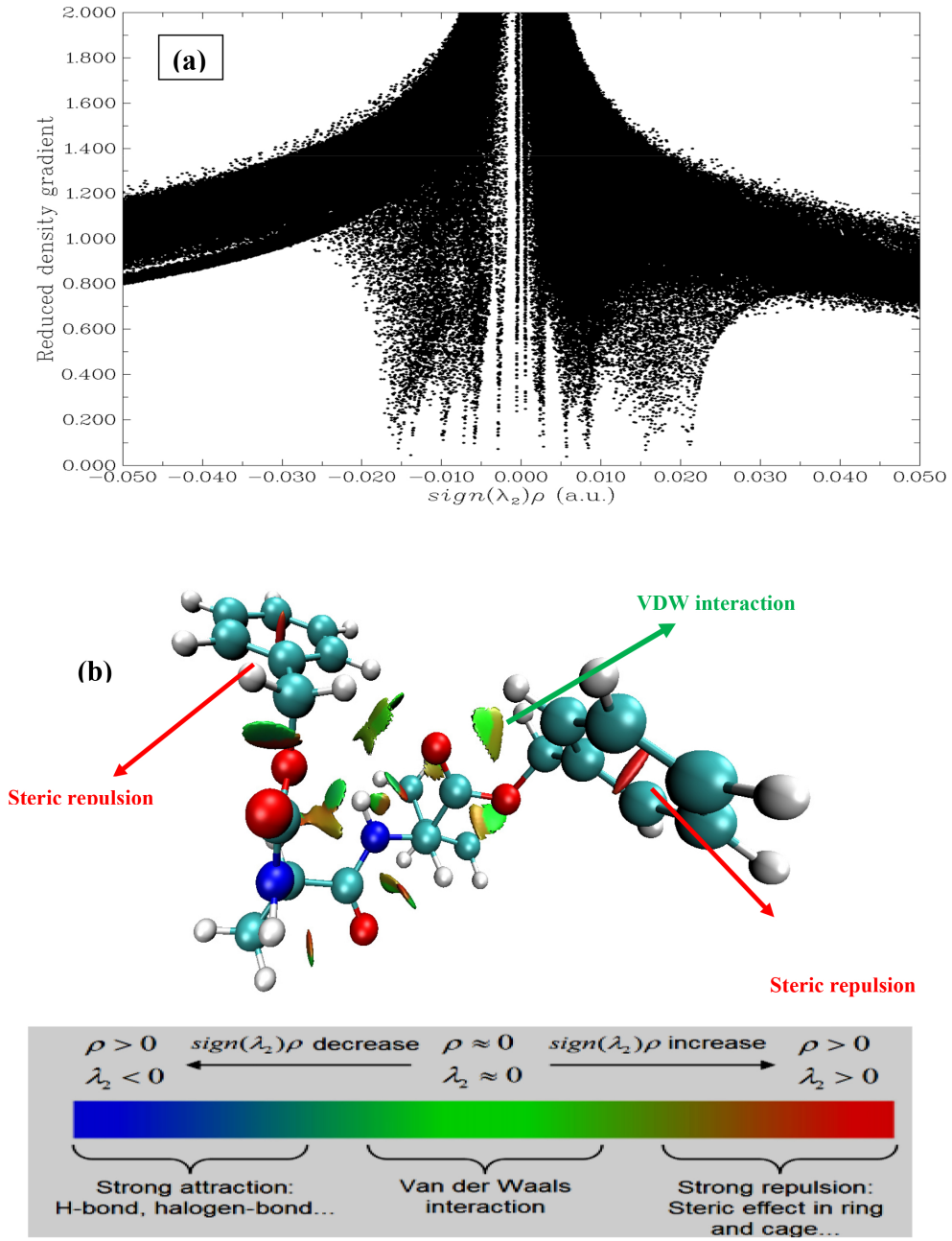

Fig. (6a, b). Reduced density gradient plot.

6.2. Reduced Density Gradient

Additionally, by determining the electron density in the molecular system, Johnson and Co-Workers [24] described the theory for weak interactions in 3D space. It has been reported that RDG is a dimensionless quantity and can be denoted as below:

$$RDG = (r) = \frac{1}{2(3\pi r^2)^{\frac{1}{3}}} \frac{\left|\Delta^2 \rho(r)\right|}{\rho(r)^{\frac{4}{3}}}$$

Low electron density regions reveal the weak interaction (b), and it was plotted by drawing electron density ρ(RDG) *vs* multiplied by the sign of λ_2. The λ_2 is helps to describe bond ($\lambda_2 < 0$) and for non-bonding ($\lambda_2 > 0$). The Multiwfn program [22] and VMD program [23] are used to calculate RDG calculation. The RDG = 0.20 lines show a strong attraction and repulsion spike in the molecule. The negative value of $(\lambda_2)\rho$ denotes the strong attraction, and the positive value of sign $(\lambda_2)\rho$ denotes the strong repulsion. Vander Waals (VdW) interactions that are close to zero are exceedingly weak. In the molecular system in Fig. (**6**), the color blue to red denotes a greater repulsive contact. The green interaction area in the CBABVE molecule indicates the existence of VdW interaction, with VdW located between C=O.....H in the oxygen atom. The title molecule has a high steric effect, which is observed in the red color and both rings.

CONCLUSION

The synthesis of a novel carbo benzyl oxy - L - alanyl - L -

valine benzyl ester (CBAVBE) is being investigated in this work. The self-assembled CBAVBE is thoroughly studied for its morphology, optical properties, and structural details using UV-Visible, UV-DRS, FT-IR, FT-Raman, HR-TEM, and FE-SEM. Computational studies are also conducted. After self-assembly, the anti-oxidant potential of carbo benzyl oxy-L-alanyl-L-valine benzyl ester is assessed. The self-assembled CBAVBE has particular chemical bonding, as demonstrated by FT-IR and Raman studies. The CBA assembly VBE is evidently well aggregated, as indicated by the obtained pictures and the FE-SEM analysis, which unequivocally verifies the fibrous nature of the CBAVBE. Although biological research is required to confirm the findings, the results were used to examine the energetically permissible zone in terms of amino acid residue. The docking indicates the binding energy strength, which is high during docking. The docking analysis suggests that the CBAVBE molecule has inhibitory action against brain and lung cancer protein, but a biological study is needed to validate the results. The docking analysis indicates that the CBAVBE molecule has inhibitory action against brain and lung cancer proteins. The chosen CBAVE has the potential to be a significant biomarker, according to antioxidant research. It is being identified as a potential paradigm for the discovery of a novel class of self-assembled peptide nano self-assemblies.

AUTHOR'S CONTRIBUTION

It is hereby acknowledged that all authors have accepted responsibility for the manuscript's content and consented to its submission. They have meticulously reviewed all results and unanimously approved the final version of the manuscript.

LIST OF ABBREVIATIONS

TMF = Trimethoxyflavone

RANKL = Receptor Activator of Nuclear Factor Kappa-B Ligand

PTH = Parathyroid Hormone

HMF = Heptamethoxyflavone

ETHICS APPROVAL AND CONSENT TO PARTICIPATE

Not applicable.

HUMAN AND ANIMAL RIGHTS

Not applicable.

CONSENT FOR PUBLICATION

Not applicable.

AVAILABILITY OF DATA AND MATERIALS

The data and supportive information are available within the article.

FUNDING

None.

CONFLICT OF INTEREST

The authors declare no conflict of interest financial or otherwise.

ACKNOWLEDGEMENTS

The authors thank RUSA 2.0 for providing the grant to carry out the part of the studies.

REFERENCES

[1] Grosser, N. Antioxidant action of L-alanine: Heme oxygenase-1 and ferritin as possible mediators. *Biochem. Biophys. Res. Commun.,* **2004**, *314*, 351-355. [http://dx.doi.org/10.1016/j.bbrc.2003.12.089] [PMID: 14733911]

[2] Szewczyk, A.; Kwiecien, I.; Grabowski, M.; Rajek, K.; Cavò, E.; Taviano, MF.; Miceli, N. Phenylalanine increases the production of antioxidant phenolic acids in ginkgo biloba cell cultures. *Molecules,* **2021**, *26*, 4965.

[3] Matsui, R.; Honda, R.; Kanome, M.; Hagiwara, A.; Matsuda, Y.; Togitani, T.; Ikemoto, N.; Terashima, M. Designing antioxidant peptides based on the antioxidant properties of the amino acid side-chains. *Food Chem.,* **2018**, *245*, 750-755. [http://dx.doi.org/10.1016/j.foodchem.2017.11.119] [PMID: 29287436]

[4] Sonklin, C.; Laohakunjit, N.; Kerdchoechuen, O. Effect of pretreatment methods on antioxidant activity of egg white hydrolysate. *PeerJ,* **2018**, *6e*, 5337.

[5] Wang, L.I.; Miller, D.P.; Sai, Y.; Liu, G.; Su, L.; Wain, J.C.; Lynch, T.J.; Christiani, D.C. Manganese superoxide dismutase alanine-to-valine polymorphism at codon 16 and lung cancer risk. *J. Natl. Cancer Inst.,* **2001**, *93*, 1-6.

[6] Jangwook, P. Jung; Joshua, Z Gasiorowski; Joel, H Collier Biotechnology and Biomedicine, Fibrillar peptide gels in biotechnology and biomedicine. *PeptideScience,* **2009**, *94*, 49-59.

[7] Won-Kyo, J. Free radical scavenging activity of a novel antioxidative peptide isolated from *in vitro* gastrointestinal digests of mytilus coruscus. *J. Med. Food,* **2007**, *1*, 197-202.

[8] Nimse, S.B. Free radicals, natural antioxidants, and their reaction mechanisms. *RSC,* **2015**, *5*, 27986-28006.

[9] Li, Chengliang.; Mora, Leticia.; Fidel, Toldr´a. Proteolysis coupled with membrane separation for the isolation of bioactive peptides from defatted smooth hound by product proteinins. *Food Res. Int.,* **2021**, *147*, 110-525.

[10] Ying Liu, Wen; Tao Zhang, Jiang; Miyakawa, Takuya ; Ming Li, Guo; ZengGu, Rui; Tanokura, Masaru Antioxidant properties and inhibition of angiotensin-converting enzyme by highly active peptides from wheat gluten. *Nature,* **2021**, *11*, 5206.

[11] Kedare, S.B.; Singh, R.P. Genesis and development of DPPH method of antioxidant assay. *J. Food Sci. Technol.,* **2011**, *48*(4), 412-422. [http://dx.doi.org/10.1007/s13197-011-0251-1] [PMID: 23572765]

[12] Eder, M.; Schlattner, U.; Wallimann, T.; Becker, A.; Kabsch, W.; Fritz-Wolf, K. Crystal structure of brain□type creatine kinase at 1.41 Å resolution. *Protein Sci.,* **1999**, *8*(11), 2258-2269. [http://dx.doi.org/10.1110/ps.8.11.2258] [PMID: 10595529]

[13] Yun, C.H.; Boggon, T.J.; Li, Y.; Woo, M.S.; Greulich, H.; Meyerson, M.; Eck, M.J. Structures of lung cancer-derived EGFR mutants and inhibitor complexes: Mechanism of activation and insights into differential inhibitor sensitivity. *Cancer Cell,* **2007**, *11*(3), 217-227. [http://dx.doi.org/10.1016/j.ccr.2006.12.017] [PMID: 17349580]

[14] Morris, G.M.; Huey, R.; Lindstrom, W.; Sanner, M.F.; Belew, R.K.; Goodsell, D.S.; Olson, A.J. AutoDock4 and AutoDockTools4: Automated docking with selective receptor flexibility. *J. Comput. Chem.,* **2009**, *30*(16), 2785-2791. [http://dx.doi.org/10.1002/jcc.21256] [PMID: 19399780]

[15] Morris, G.M.; Huey, R.; Olson, A.J. Using autodock for ligand-receptor docking. *Curr. Protoc. Bioinformatics,* **2008**.

[16] Ruth, H.; Garrett, M.M.; Arthur, J.O.; David, S.G. A semiempirical free energy force field with charge-based desolvation. *J. Comput. Chem.,* **2007**, *28*, 1145-1152. [http://dx.doi.org/10.1002/jcc.20634] [PMID: 17274016]

[17] Garrett, M.M.; David, S.G.; Robert, S.H.; Ruth, H.; William, E.H.; Richard, K.B.; Arthur, J.O. Automated docking using a Lamarckian genetic algorithm and an empirical binding free energy function. *J. Comput. Chem.,* **1998**, *19*, 1639-1662.

[http://dx.doi.org/10.1002/(SICI)1096-987X(19981115)19:14<1639::AID-JCC10>3.0.CO;2-B]

[18] Frisch, M.J.; Trucks, G.W.; Schlegel, H.B.; Scuseria, G.E. *Gaussian-09, Revision A.02, Gaussian*; Wallingford CT, **2009**.

[19] De Lano, W. L. *The Py MOL Molecular Graphics System*; De Lano Scientific: San Carlos, CA USA, **2002**.

[20] Kramer, B.; Rarey, M.; Lengauer, T. Evaluation of the FLEXX incremental construction algorithm for protein-ligand docking. *Proteins,* **1999**, *37*(2), 228-241. [http://dx.doi.org/10.1002/(SICI)1097-0134(19991101)37:2<228::AID-PROT8>3.0.CO;2-8] [PMID: 10584068]

[21] Sebastian A, S.; Sylvestre, S.; Sundaraganesan, N.; Karthikeyan, N.; Silvan, S. Conformational analysis, molecular structure, spectroscopic, NBO, reactivity descriptors, wavefunction and molecular docking investigations of 5,6-dimethoxy-1-indanone: A potential anti Alzheimer's agent *Heliyon,* **2022**, 2406-8440.

[22] Lu, T.; Chem, F. A multifunctional wave function analyser. *J. Comput. Chem.,* **2012**, •••, 43.

[23] Humphrey, W.; Dalke, A.; Schulten, K. VMD: Visual molecular dynamics. *J. Mol. Graph.,* **1996**, *14*, 33-38.

[24] Johnson, E. R.; Keinan, S.; Sanchez, P.M.; Garcia, J.C.; Cohen, A.J.; Yong, W. Revealing noncovalent interactions. *J. Am. Chem. Soc.,* **2010**, *132*, 6498-6506.